

RECENT DEVELOPMENTS IN THERMOELECTRIC METROLOGY AT NIST

¹W. Wong-Ng, ¹J. Martin, ¹E. L. Thomas, ¹M. Otani, ¹N. Lowhorn, ¹M. Green, ¹G. Liu, ¹Y.G. Yan, ¹J. Hatrick-Simpers, and ²T. Tran
¹MSEL, NIST, Gaithersburg, MD 20899
²NSWC, Bethesda MD 20817

ABSTRACT

We have recently developed several important thermoelectric metrologies at NIST. First, a low temperature (10 K to 390 K) Seebeck coefficient Standard Reference Material (SRMTM), Bi₂Te₃, which is crucial for inter-laboratory data comparison and for instrument calibration, has been produced. Second, to accelerate thermoelectric material exploration, a high-throughput thermoelectric screening system for combinatorial thin films was developed. The screening device for thermoelectric power factor ($S^2\sigma$; S = Seebeck coefficient, σ = electrical conductivity) allows us to measure σ and S of over 1000 sample-points within 6 hours. The thermal effusivity screening system using the frequency domain thermoreflectance technique allows us to determine thermal conductivity of combinatorial films, conventional films and bulk materials with high efficiency, i.e. 1000 data points within 6 hours. Third, a flexible and reliable instrument to measure high temperature Seebeck coefficient and resistivity is under development. This tool allows the minimization of a number of measurement uncertainties that contribute to the overall systematic errors.

INTRODUCTION

Thermoelectric materials have demonstrated potential for both waste heat recovery and solid-state refrigeration applications. The efficiency and performance of thermoelectric power generation or cooling is related to the dimensionless figure of merit (ZT) of the thermoelectric materials, given by $ZT = S^2\sigma T/\kappa$, where T is the absolute temperature, S is the Seebeck coefficient, σ is the electrical conductivity ($\sigma=1/\rho$, ρ is electrical resistivity), and κ is the thermal conductivity [1, 2]. ZT is directly related to the performance of a thermoelectric material and is the reference by which these materials are judged. The Seebeck coefficient is an important indicator for power conversion efficiency. Thermoelectric materials with desirable properties (i.e., high $ZT \gg 1$), are characterized by high electrical conductivity, high Seebeck coefficient, and low thermal conductivity, and will have widespread applications.

Until recently, only a small number of materials have been found to have practical industrial applications because of generally low thermoelectric efficiencies. Increased attention to research and development of thermoelectric materials has been partly due to the dramatic increase of the ZT values of materials being discovered in bulk and thin film form [3, 4, 5]. Additional novel materials include quantum well films [6] and quantum dot films [7] that have been reported to yield ZT as high as 2.5.

The goal of this paper is to summarize our recent efforts on the development of thermoelectric metrology, including a low temperature Seebeck coefficient standard reference material (SRMTM), a screening tool suite for screening the thermoelectric properties of combinatorial films, and a novel measurement tool for high temperature Seebeck coefficient and resistivity.

LOW TEMPERATURE SEEBECK COEFFICIENT STANDARD REFERENCE MATERIAL (10K to 390K)

The main mission of NIST is to promote U.S. innovation and industrial competitiveness by advancing measurement science, standards, and technology. The development of standard reference materials (SRMs™) for thermoelectric research is essential for U.S. industry. Although the viability of vehicular thermoelectric converters has been demonstrated on a research-scale, for large-scale manufacturing accurate measurements of thermoelectric properties, standardized metrologies are needed. Furthermore, the availability of standard reference materials will validate measurement accuracy, leading to a better understanding of the structure/property relationships and the underlying physics of new and improved thermoelectric materials.

SRMs™ are available for thermal conductivity and electrical conductivity (NIST SRM™ 8420/8421-electrolytic iron and 8424/8426-graphite), however, a moderate to high Seebeck coefficient standard reference material does not exist. To enable inter-laboratory data comparison and validation of measurements, we have initiated a project to develop Seebeck coefficient SRMs™ for both low temperature and high temperature applications. Recently, we have completed the certification of a low temperature Seebeck coefficient standard reference material (SRM 3451). This project began about three years ago. A round-robin measurement survey was first conducted to determine the appropriate material and to examine different measurement techniques. Two candidate materials, constantan and undoped-Bi₂Te₃ were circulated between 12 laboratories actively involved in thermoelectric research. The details and results from this survey are presented elsewhere [8, 9]. As a result of the round robin study, Bi₂Te₃ was chosen as the prototype SRM. The SRM material, provided by Marlow Industries, is a bar-shaped sample of Te-doped Bi₂Te₃ [(Bi_{1.998}Tc_{0.002})Te₃] which measures (3.5 mm x 2.5 mm x 8.0 mm).

The Seebeck coefficient is defined as the ratio of the Seebeck voltage (ΔV) to the applied temperature gradient (ΔT) [10]. The basic concept of a typical Seebeck measurement only requires the creation of a ΔT , measurement of the ΔT and resulting ΔV . For our certification measurements, we used two different measurement techniques which used completely different measurement software while sharing much of the same hardware. The primary technique was a custom (with third party instruments), steady-state, sweep technique using a modified Quantum Design Physical Property Measurement System (PPMS) (Model PPMS-9)*. In this technique, the sample was held at a constant temperature while a range of ΔT values were created and the corresponding ΔV values measured. Graphing this data produced a line from which the slope yielded the Seebeck coefficient. Custom software was written using LabVIEW [11] to automate the measurements and data collection. The secondary technique used the standard PPMS Thermal Transport Option (TTO) Seebeck measurement method. This method monitors the ΔT and ΔV along the sample while supplying a continuous ac heat pulse to one end and slowly varying the sample temperature. The steady-state values for ΔT and ΔV are found by extrapolating the data from a relatively short heat pulse.

Ten samples were selected randomly from the SRM batch of 390 received from Marlow Industries. The details of the sample mounting and calibration of thermometers are discussed elsewhere [12-14]. Five of the samples were measured twice using the primary technique. The other five samples were measured once with this same technique. All ten samples were measured once using the secondary technique.

In the primary technique, the Seebeck coefficient values were measured at 32 temperature values for each of the 10 samples. The Seebeck coefficient ΔV data from the secondary

TTO technique consists of 10 measurement curves but with many more temperature values as compared to the data from the primary technique. These TTO data were analyzed by focusing on the 32 temperature values and use interpolated values for comparison and combined mean analysis with the primary data [15].

The data from the two measurement techniques are very similar, as evidenced from a t-test based on the two data sets at each of the 32 temperature values [16]. The primary and secondary SRM data are therefore combined to produce a final mean curve with a 95 % confidence band (Fig 1). The uncertainty values include both the random and systematic errors (from the measurements of ΔV , ΔT and T). We can also fit a parametric model to the final mean value by a 4th-order polynomial,

$$m(t) = a_0 + a_1 t + a_2 (t - 200)^2 + a_3 (t - 200)^3 + a_4 (t - 200)^4. \quad (1)$$

Using the least squares estimation, the parameters a_0, a_1, a_2, a_3, a_4 are identified as -27.55699, -0.7653341, 0.00201416, 7.443016e-006, and -5.758658e-009. This equation serves as an interpolation model for obtaining Seebeck coefficient values in between the measurement range of the 32 certified values, from 10 K to 390 K. This SRM will be available in 2010.

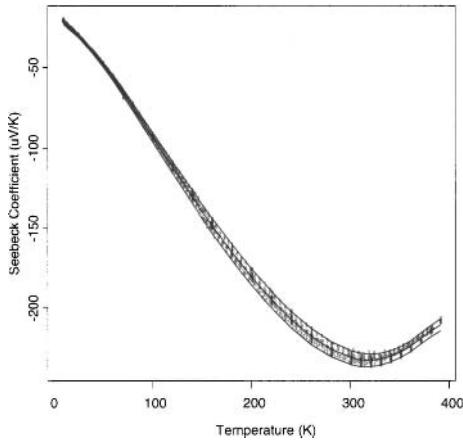


Fig. 1. Plots of data from the primary technique (dark pluses in intervals), secondary technique (dots), and final mean with a 95% confidence (solid lines in black). Both random and systematic errors are included in this plot.

A SUITE OF SCREENING TOOLS FOR COMBINATORIAL FILMS

For large-scale applications of thermoelectric technology, continued efforts to identify novel materials and to optimize the properties of existing materials are crucial. The combinatorial state-of-the-art synthesis approach is an efficient technique to systematically investigate the thermoelectric properties as a function of composition in complex multi-component systems. This method typically involves fabricating film libraries with varying compositions between two or three different materials on a substrate using physical vapor deposition techniques, followed by evaluating the film libraries with high-throughput screening tools [17-19]. We have developed a high-throughput screening system for thermoelectric material exploration using combinatorial films prepared with a continuous spread of compositions. This system consists of a power factor screening tool and a thermal conductivity screening tool [20].

Power Factor Screening tool

The high-throughput power factor screening tool that we developed can be used to measure electrical conductivity and Seebeck coefficient [21, 22]. Measurements are fully automated by a computer. The salient features of the power factor screening tool consist of a probe to measure Seebeck coefficient and electric conductivity, an automated translation stage to scan the probe in the x - y - z directions, and various voltage measuring instruments. The measurement probe consists of four gold-plated spring probes as sample contacts, a heater to generate temperature differences between two of the spring probes, two thermometers to measure the temperature of these probes, two insulators, and two copper plates, as shown in Fig. 2. To achieve accurate Seebeck coefficient measurements, a spring probe is directly placed on each copper plate to ensure low thermal resistance between the probe and the copper plate. The other spring probe is attached on the insulator. The four probes can be arranged either in a square array or in a linear fashion. A thermometer is attached on each copper plate and a heater is attached on one of the copper plates. Electrical conductivity is measured by the conventional 4-probe method (van der Pauw method [23]). All Seebeck coefficient measurements were conducted at room temperature and at $\Delta T = 4.1$ K. It takes about 20 seconds to measure both electric conductivity and Seebeck coefficient for each sample point. This probe allows us to measure electric conductivity and Seebeck coefficient of over 1000 sample points within 6 hours.

The screening tool has been used to evaluate the homogeneity of two industrially important samples (in the form of rectangular bars of approximately 2.5 mm x 2.5 mm x 10 mm). The first sample is a Type-I clathrate, $\text{Ba}_8(\text{Ni},\text{Pt},\text{Pd},\text{Zn})\text{Ga}_{13}\text{Ge}_{46}$ [24] (Fig. 3), and the second sample is a triple-filled skutteruide ($\text{Ba},\text{Yb})\text{Sb}_4\text{Co}_{12}$ [25, 26] (Fig. 4). $\text{Ba}_8(\text{Ni},\text{Pt},\text{Pd},\text{Zn})\text{Ga}_{13}\text{Ge}_{46}$ has an "open" structure that can host guest atoms inside the crystallographic voids. The rattling Ba atoms inside the large Ge/Ga cages scatter phonons and thus reduce thermal conductivity. The $(\text{Ba},\text{Yb})\text{Sb}_4\text{Co}_{12}$ skutteruide has a cubic structure that consists of six 4-membered Sb-rings that are almost parallel to the cell edges. The two large voids in the unit cell can be filled with rattling atoms (in the present compound, a mix of Ba and Yb ions). Table I gives the systematic measurement results of the Seebeck coefficient values at continuously changing positions on the two samples. The measurement positions are parallel to the thermal gradient. Each data point was collected after a 30 second stabilization period. A total of 13 scanned data points on $\text{Ba}_8(\text{Ni},\text{Pt},\text{Pd},\text{Zn})\text{Ga}_{13}\text{Ge}_{46}$ gives an average Seebeck coefficient value of $-67 \mu\text{V}/\text{K}$ with a 4.5 % ($3.0 \mu\text{V}/\text{K}$) standard deviation. Based on the screening of 16 data points, the average Seebeck

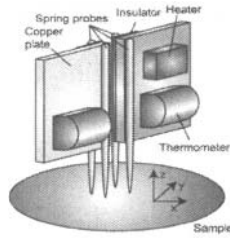


Fig. 2. Schematic of the screening probe to measure electrical conductivity and Seebeck coefficient.

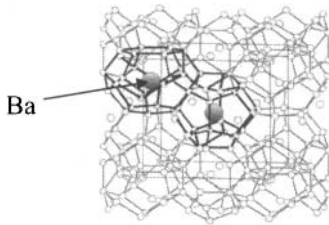


Fig. 3. The type-I clathrate crystal structure. Outlined are the two different polyhedra that form the unit cell with the dodecahedron (20-atom cage) in the center and the tetrakaidecahedron (24-atom cage) to the upper left. The Ba atoms inside the polyhedra are shown.

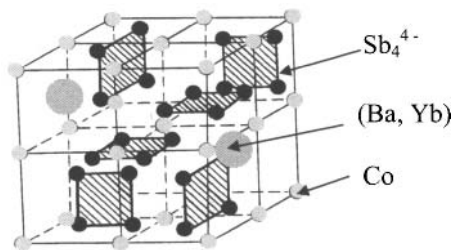


Fig. 4. Structure of the skutterudite $(\text{Ba, Yb})\text{Sb}_4\text{Co}_{12}$ showing the Sb_4 rings and the voids in the unit cell where the mixed (Ba, Yb) ions reside.

Table I. Seebeck coefficient of the (Ba, Yb)Sb₄Co₁₂ and Ba₈(Ni,Pt,Pd,Zn)Ga₁₃Ge₄ samples obtained using the power factor screening tool.

Position (μm)	(Ba, Yb)Sb ₄ Co ₁₂		Ba ₈ (Ni,Pt,Pd,Zn)Ga ₁₃ Ge ₄	
	V	S	V	S
0	-0.486	-128	-0.218	-57
500	-0.501	-132	-0.232	-61
1000	-0.488	-128	-0.253	-67
1500	-0.479	-126	-0.245	-64
2000	-0.482	-127	-0.247	-65
2500	-0.5	-132	-0.237	-62
3000	-0.484	-127	-0.219	-58
3500	-0.482	-127	-0.238	-63
4000	-0.478	-126	-0.246	-65
4500	-0.485	-128	-0.233	-61
5000	-0.497	-131	-0.246	-65
5500	-0.487	-128	-0.24	-63
6000	-0.474	-125	-0.254	-67
6500	-0.49	-129		
7000	-0.482	-127		
7500	-0.467	-123		

coefficient for (Ba, Yb)Sb₄Co₁₂ is -128 μV/K with a 2 % (2.37 μV/K) standard deviation. Therefore we conclude that these are essentially homogenous samples, as no systematic change in Seebeck coefficient was observed as a function of position.

Recently technologically important LaMO₃ (*M* = Co, Ni) materials have been selected to generate a single-crystalline continuous-spread binary combinatorial thin film library. A film was deposited onto a 45 mm x 5 mm of LaAlO₃ (100) substrate by short duration KrF excimer laser beam pulses (25 ns) of LaCoO₃ and LaNiO₃ targets via pulsed laser deposition inside a vacuum chamber with a *p*_{O₂} = 13.3 Pa at *T* = 600 °C. X-ray diffraction data obtained via a Bruker General Area Detection Diffraction System revealed that the film was highly crystalline with a cubic structure, and lattice parameters ranging from 3.8268 Å (Co end) to 3.8792 Å (Ni end). The resulting structural diagram was correlated with measurements of thermoelectric property variations as a function of wafer position using the screening tool. Preliminary TE data are shown in Fig. 5. Measurements of the Seebeck coefficient (*α*) show a positive to negative transition as a result of the addition of Ni, which affects the nature of the charge carriers from holes to electrons. The electrical resistivity (*ρ*) of the film shows a substantial decrease as more Ni is substituted on the Co site. The thermoelectric behavior of the La(Co,Ni)O₃ binary film is similar to the behavior observed in previous studies of the bulk counterparts [27].

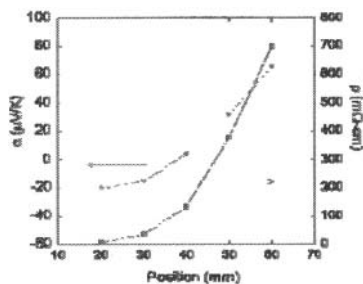


Fig. 5. Room temperature Seebeck coefficient and electrical resistivity data for the $\text{La}(\text{Co}, \text{Ni})\text{O}_3$ binary film. Ni-content decreases as position changes from 20 to 60 mm.

We have also applied the screening tool to a $(\text{Ca}_{1-x-y}\text{Sr}_x\text{La}_y)_3\text{Co}_4\text{O}_9$ ternary composition-spread film using $\text{Ca}_3\text{Co}_4\text{O}_9$, $\text{Ca}_2\text{LaCo}_4\text{O}_9$, and $\text{Ca}_2\text{SrCo}_4\text{O}_9$ as targets [21, 22]. Figure 6 gives the results of the power factor screening of this system (depicted as a conventional ternary diagram). It is clear that the power factor data reach a maximum between the Sr-rich region and the La-rich region. Substitution of the trivalent La^{3+} for the divalent Ca^{2+} is expected to decrease the hole concentration, leading to increasing Seebeck coefficient in the La-rich region. On the other hand, substitution of Sr^{2+} for Ca^{2+} leads to an increase of electrical conductivity and an insignificant change of Seebeck coefficient. This is because the substitution of a larger divalent Sr^{2+} cation for a smaller divalent Ca^{2+} cation would not change the carrier concentration but it would change the carrier mobility by lattice deformation.

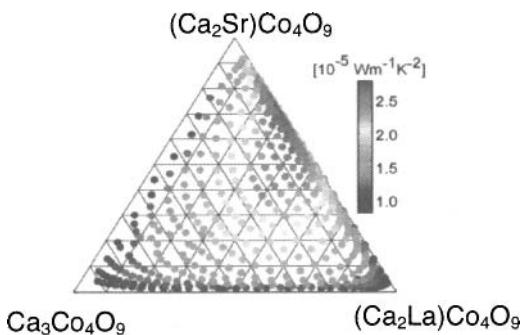


Fig. 6. Power factor of the composition-spread $(\text{Ca}_{1-x-y}\text{Sr}_x\text{La}_y)_3\text{Co}_4\text{O}_9$ film ($0 < x < 1/3$ and $0 < y < 1/3$).

Thermal conductivity screening tool (Frequency-domain thermoreflectance technique)

A scanning thermal effusivity measurement system using the frequency domain thermoreflectance technique and periodic heating has been developed [20]. The thermoreflectance technique is based on the relationship between the change in the optical reflection coefficient of a material and the change in its temperature. By using a metal for the film layer, this method can measure thermal effusivity of ceramics, metals, glass, and plastics. The thermal effusivity measurement system using the frequency domain thermoreflectance technique can rapidly and locally (10 micrometer spot size) measure the thermal effusivity of combinatorial (composition-spread) films.

Figure 7 gives a schematic of the scanning thermal effusivity frequency system that includes two laser diodes, a compensating network, a voltage source heater, and a x-y-z axis automated sample stage driven by a motor driver. The sample, which is a thermoelectric film or a bulk sample with a smooth surface, is first coated with a thin molybdenum layer (usually about 100 nm thick), then is locally heated by an intensity-modulated heating laser; the thermal response of the film is detected by the reflected beam of a second (probe) laser. The reflected probe signal is detected by a balance detector. The amplitude and phase difference between signal and reference signal from the pulse generator are obtained by a lock-in amplifier.

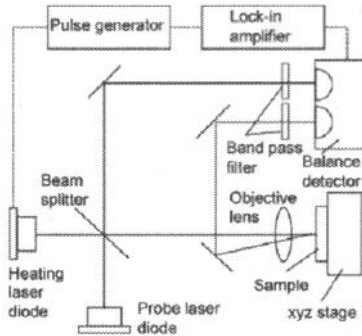


Fig. 7. Schematic diagram of the thermal effusivity screening system (frequency domain thermoreflectance technique)

The thermal effusivity b can be derived from the phase lag, δ , between the thermoreflectance and the heating laser signals. Thermal effusivity is related to thermal conductivity as $b = (\kappa c \rho)^{1/2}$, where c is the specific heat, ρ is the density, and κ is thermal conductivity. By choosing the modulated frequency of 1 MHz, we obtained a calibration curve of the phase lag of five bulk samples of which the thermal effusivity values are known: SiO₂, SrTiO₃, LaAlO₃, Al₂O₃, and Si. The linear dependence of the phase lag on thermal effusivity of these five compounds can be expressed in the following equation,

$$b = -402.34 \delta + 26352, \quad (2)$$

where b is the thermal effusivity. If the δ value for an unknown material can be measured experimentally, one can estimate b using equation (2).

We successfully estimated the thermal conductivity value for a 800nm/(100nm Mo) thick conventional $\text{Ba}_2\text{YCu}_3\text{O}_{6+x}$ film on a SrTiO_3 substrate. Using equation (1), the thermal effusivity was estimated to be $1370 \text{ Js}^{1/2}\text{M}^{-2}\text{K}^{-1}$ ($\delta = 62.1^\circ$). The thermal conductivity of the $\text{Ba}_2\text{YCu}_3\text{O}_{6+x}$ film was then determined ($c = 430 \text{ J.kg}^{-1}\text{K}^{-1}$ [28], and $\rho = 6.38 \text{ g.cm}^{-3}$ [29]) to be $12.0 \text{ Jm}^{-1}\text{K}^{-1}\text{s}^{-1}$, which agrees reasonably well (within 10 %) with the reported value of $12.9 \text{ Jm}^{-1}\text{K}^{-1}\text{s}^{-1}$ [28].

To assess the application of the tool for 2-dimensional screening, we determined the δ values of a Si sample in the yz -direction (with a 100 nm-thick Mo metallic film on the surface). Using equation (2) with the c , ρ values of $0.713 \text{ Jg}^{-1}\text{K}^{-1}$ [30] and 2.3290 g.cm^{-3} [30], respectively, and the measured δ values, we obtained the thermal effusivity and thermal conductivity values of the Si sample in an area of approximately $1 \text{ mm} \times 1 \text{ mm}$ in increments of $100 \mu\text{m}$. Figure 8 shows the two dimensional 10×10 data net of the thermal conductivity values. The resulting average κ is $(1.65 \pm 0.148) \text{ Wcm}^{-1}\text{K}^{-1}$, which is within 8 % of the literature reported value of $1.56 \text{ Wcm}^{-1}\text{K}^{-1}$ [30]. Using this tool, we plan to study the thermal properties of combinatorial film systems in the future.

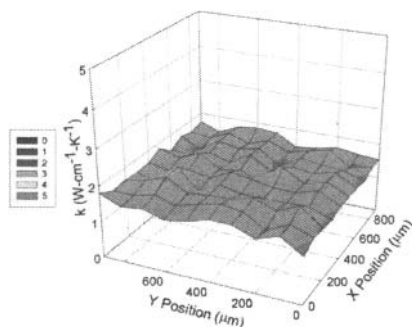


Fig. 8. Thermal conductivity data of the Si sample in an area of approximately $1 \text{ mm} \times 1 \text{ mm}$ in increments of $100 \mu\text{m}$ in both y and z directions.

High temperature power factor measurement tool

NIST is developing a novel high temperature metrology apparatus to concurrently measure the Seebeck coefficient and resistivity. This apparatus is capable of *in situ* comparison and evaluation of various contact and characterization methodologies. Therefore the success of this instrumentation not only expands the flexibility with respect to specimen size and geometry, but also allows for validation of different arrangements and methodologies. Some key features include: 1) The sample probe is machined from high purity tungsten to accommodate both parallelepiped and disk shaped specimens, in both transverse and longitudinal configuration; 2) The thermocouple probe distance is automatically adjusted based on the specimen length. Special precautions have also been implemented to reduce the influence of secondary voltage contributions on thermocouple readings; 3) Dual, non-inductive spiral wire heaters on each ceramic jacket allow for bipolar thermal gradients and a better zero-gradient for resistivity measurements; 4) The specimen temperature is maintained and adjusted using an infrared furnace consisting of gold parabolic reflector IR tubes for thermal stability with both axial and longitudinal profile consistency; and 5) The use of multiple nanovoltmeters to eliminate the smearing of the Seebeck coefficient when using gradient sweep or multiple static gradient techniques.

FUTURE DEVELOPMENTS

For applications in energy conversion industries including the automotive industry, it is important to have a high temperature Seebeck coefficient SRM. Upon the completion of the high temperature Seebeck coefficient measuring tool, we plan to work with the international thermoelectric research community to develop a high temperature Seebeck coefficient SRM.

Our continuing development of the power factor screening tool for the thermoelectric combinatorial films focuses on the improvement of its performance. There are three limitations to the current screening tool configuration [21, 22]. First, it is difficult to measure materials with low (i.e., $\leq 10^{-1} (\Omega\text{cm})^{-1}$ for a 200 nm thin film) electrical conductivity and low ($\approx 5\mu\text{V/K}$) absolute value of Seebeck coefficient due only to limitations of the homemade current source and voltage meter. Although these limitations do not hamper our ability to screen thermoelectric materials, we could extend our measurement capability by upgrading those two components. Second, the spatial resolution of our screening tool is about 2 mm, corresponding to the distance between two spring probes. If the electrical conductivity of the sample drastically changed over a very short length scale, measurements at a sample point might be affected by its neighbors. We plan to improve this resolution. Third, measurements can be carried out only at room temperature at present. We plan to develop an improved instrument that is capable of high temperature (μp to 600 °C) measurement.

FOOTNOTES

* Certain commercial equipment, instruments, or materials are identified in this paper in order to specify the experimental procedure adequately. Such identification is not intended to imply recommendation or endorsement by the National Institute of Standards and Technology, nor is it intended to imply that the materials or equipment identified are necessarily the best available for the purpose.

REFERENCES

- ¹ T.M. Tritt, Thermoelectrics Run Hot and Cold, *Science*, **272**, 1276-1277 (1996).
- ² K.F. Hsu, S. Loo, F. Guo, W. Chen, J.S. Dyck, C. Uher, T. Hogan, E.K. Polychroniadis, and M.G. Kanatzidis, Cubic $\text{AgPb}_m\text{SbTe}_{2-m}$: Bulk Thermoelectric Materials with High Figure of Merit, *Science*, **303**, 818-821 (2004).
- ³ R. Venkatasubramanian, E. Siivola, T. Colpitts, and B. O'Quinn, Growth of one-dimensional Si/SiGe heterostructures by thermal CVD, *Nature*, **413**, 597-602 (2001).
- ⁴ S. Ghamaty, and N.B. Eisner, "Development of Quantum Well Thermoelectric films, Proceedings of the 18th International Conference on Thermoelectrics, Baltimore, MD, pp. 485-488 (1999).
- ⁵ M.S. Dresselhaus, G. Chen, M.Y. Tang, R.G. Yang, H. Lee, D.Z. Wang, Z.F. Ren, J.P. Fleurial, and P. Gogna, Enhanced Thermopower in PbSe Nanocrystal Quantum Dot Superlattices, *Adv. Mater.*, **19**, 1043-1053 (2007).
- ⁶ R. Funahashi, S. Urata, and M. Kitawaki, Exploration of n-type oxides by high throughput screening, *Appl. Surf. Sci.*, **223**, 44-48 (2004).
- ⁷ T. He, J.Z. Chen, T.G. Calvarese, M.A. Subramanian, Thermoelectric properties of $\text{La}_{1-x}\text{A}_x\text{CoO}_3$ (A = Pb, Na), *Solid State Sciences*, **8**, 467-469 (2006).
- ⁸ N. D. Lowhorn, W. Wong-Ng, Z. Q. J. Lu, W. Zhang, E. Thomas, M. Otani, M. Green, T. N. Tran, C. Caylor, N. Dilley, A. Downey, B. Edwards, N. Elsner, S. Ghamaty, T. Hogan, Q. Jie, Q. Li, J. Martin, G. Nolas, H. Obara, J. Sharp, R. Venkatasubramanian, R. Willigan, J. Yang, and T. Tritt, Round-Robin Studies of Two Potential Seebeck Coefficient Standard Reference Materials, *Appl. Phys. A, (Materials Science & processing)*, **94**, 231-234 (2009).
- ⁹ Z. Q. J. Lu, N. D. Lowhorn, W. Wong-Ng, W. Zhang, E. Thomas, M. Otani, M. Green, T. N. Tran, C. Caylor, N. Dilley, A. Downey, B. Edwards, N. Elsner, S. Ghamaty, T. Hogan, Q. Jie, Q. Li, J. Martin, G. Nolas, H. Obara, J. Sharp, R. Venkatasubramanian, R. Willigan, J. Yang, and T. Tritt, Statistical Analysis of two Candidate Materials for a Seebeck Coefficient Standard Reference Material (SRMTM), *J. Res. Nat'l Inst. Stand & Tech.*, **114** (1), 37-55 (2009).
- ¹⁰ T. M. Tritt and M. A. Subramanian, Thermoelectric Materials, Phenomena, and Applications: A Bird's Eye View, *Mater. Res. Soc. Bull.*, **31**, 188-194 (2006).
- ¹¹ LabVIEW is a programming language produced by National Instruments which is commonly used for experiment control.
- ¹² N. D. Lowhorn, W. Wong-Ng, Z.Q. Lu, E. Thomas, M. Otani, M. Green, N. Dilley, J. Sharp, and T. N. Tran, Development of a Seebeck Coefficient Standard Reference Material, *Appl. Phys A*, **96**, 511-514 (2009).
- ¹³ NIST-traceable primary Cernox thermometer for low temperatures
- ¹⁴ NIST-traceable platinum thermometer for temperatures greater than 100 K
- ¹⁵ Splus is a trademark of Insightful Corporation. Mention of a software product in this paper is only to illustrate and to make explicit the statistical procedures used in our data analysis, and does not imply in anyway the endorsements of NIST, nor that the product is the best available for the purpose.
- ¹⁶ G.A.F. Seber. *Linear Regression Analysis*, Chapter 8. Wiley, New York (1977).
- ¹⁷ R. B. Van Dover, L. F. Schneemeyer, R. M. Fleming, Discovery of a useful thin-film dielectric using a composition-spread approach, *Nature*, **392**, 162 (1998).
- ¹⁸ T. Fukumura, M. Ohtani, M. Kawasaki, Y. Okimoto, T. Kageyama, T. Koida, T. Hasegawa, Y. Tokura, H. Koinuma, Rapid construction of phase diagram for doped Mott insulators with a composition-spread approach, *Appl. Phys. Lett.*, **77**, 3426-3428 (2000).

- ¹⁹H. M. Christen, S. D. Silliman, and K. S. Harchavardhan, Continuous compositional-spread technique based on pulsed-laser deposition and applied to the growth of epitaxial films, *Rev. Sci. Instrum.*, **72**, 2673-2678 (2001).
- ²⁰M. Otani, E. Thomas, W. Wong-Ng, P. K. Schenck, K.-S. Chang, N. D. Lowhorn, M. L. Green, and H. Ohguchi, A High-throughput Screening System for Thermoelectric Material Exploration Based on a Combinatorial Film Approach, *Jap. J. Appl. Phys.*, **48**, 05EB02 (2009).
- ²¹M. Otani, N.D. Lowhorn, P.K. Schenck, W. Wong-Ng, and M. Green, A High-throughput thermoelectric Screening Tool for Rapid Construction of Thermoelectric Phase Diagrams, *Appl. Phys. Lett.*, **91**, 132102-132104 (2007).
- ²²M. Otani, K. Itaka, W. Wong-Ng, P.K. Schenck, and H. Koinuma, Development of high-throughput thermoelectric tool for combinatorial thin film libraries, *Appl. Surface Science*, **254**, 765-767 (2007).
- ²³L.J. van der Pauw, *Philips Tech. Rev.*, A Method of Measuring the Resistivity and Hall Coefficient on Lamellae of Arbitrary Shape, **20**, 220-224, (1958).
- ²⁴X. Shi, H. Kong, C.-P. Li, C. Uher, J. Yang, J.R. Salvador, H. Wang, L. Chen, and W. Zhang, Low thermal conductivity and high thermoelectric figure of merit in n-type $Ba_xYb_yCo_4Sb_{12}$ double-filled skutteruide, *Appl. Phys. Lett.* **92**, 182101 (2008).
- ²⁵X. Shi, J.R. Salvador, J. Yang, and H. Wang, Thermoelectric Properties of n-Type Multiple-Filled Skutterudites, *J. Electronic Mater.* **38**(7), 930-933 (2009).
- ²⁶C. Uher, Skutterudites: Prospective Novel Thermoelectrics in Semiconductors and Semimetals, *Semiconductors & Semimetals*, **69**, 139-253 (2001).
- ²⁷R. Robert, L. Bocher, M. Trottmann, A. Reller, and A. Weidenkaff, Synthesis and high-temperature thermoelectric properties of Ni and Ti substituted $LaCoO_3$, *J. Solid State Chem.*, **179**, 3893-3899 (2006).
- ²⁸T. Yagi, N. Taketoshi, and H. Kato, Distribution analysis of thermal effusivity for sub-micrometer YBCO thin films using thermal microscope, *Physica C*, **412-414**, 1337-1342 (2004).
- ²⁹W. Wong-Ng, R.S. Roth, L.J. Swartzendruber, L.H. Bennett, C.K. Chiang, F. Beech, and C.R. Hubbard, X-ray powder characterization of $Ba_2YCu_3O_{7-x}$, *Adv. Ceram. Mater.*, Vol. **2**(3B), *Ceramic Superconductors*, ed. W. J. Smothers, Am. Ceram. Soc., Westerville, OH, p. 565 (1987).
- ³⁰Robert Hull, Editor, *Properties of Crystalline Silicon*, INSPEC, The Institution of Electrical Engineers, London, p. 165 (1999).